Prediction of Thermocline Zone Development at the Beginning of Dynamic Processes in Single Storage Tanks with Liquid Media

Rocío Bayón[1, a)] and Esther Rojas[1, b)]

[1] *Thermal Storage and Solar Fuels Unit. CIEMAT-PSA. Av. Complutense 40, 28040 Madrid (Spain)*
[a)]*Corresponding author: rocio.bayon@ciemat.es*
[b)]*esther.rojas@ciemat.es*

Abstract. Thermocline development in tanks with liquid storage media is strongly affected by both turbulences and fluid mixing, which take place mainly at the inlet. The occurrence of these phenomena leads to an increase of thermocline zone thickness, which implies that less energy can be extracted from the storage tank. Although this is an important issue, the majority of simulation models for single tanks do not consider turbulence and mixing phenomena so they are not able to predict how thermocline zone develops at the beginning of dynamic processes. In this paper the effect of turbulence and mixing phenomena in the initial formation of thermocline has been evaluated by analyzing experimental data found in the literature for single tanks with different inlet configurations. This effect has been quantified by means of an eddy function, which has been introduced as a correction to the fluid diffusivity. The dependence of this function with the Richardson number at tank inlet has been discussed for the thermocline tanks that have been analyzed. However, still many questions remain open since more systematic experiments with different inlet configurations and working conditions should are required.

INTRODUCTION

Temperature evolution along a storage tank with only liquid storage medium is strongly affected by both turbulences and fluid mixing, which take place at fluid inlet. The occurrence of these phenomena defines the initial thermocline zone thickness, and hence, the useful energy that can be provided by the storage system. Therefore it is important to know the effect of turbulences and mixing in the development of thermocline zone. The majority of simulation models for single tanks do not consider this kind of phenomena so that the prediction of thermocline zone development at the beginning of dynamic process is an issue that still remains unsolved.

Different authors have attempted to include turbulence and mixing effects in their simulation models for single tanks with water [1, 2, 3, 4, 5]. Zurigat et al. [1], from Oklahoma State University, proposed including them through an effective diffusivity factor, ε_{eff}, linked to the thermal diffusivity, α, in the thermal energy equation (see Table 1). For laminar flow, ε_{eff} is equal to one but for turbulent flow, ε_{eff} is much greater than unity, which is equivalent to say that thermal diffusivity is magnified by turbulences by a factor of ε_{eff}. Additionally, and based on Oppel's results [6], ε_{eff} factor is proposed to vary spatially from a maximum at the tank inlet, ε_{eff}^{in}, to a minimum at the tank outlet by means of a decreasing hyperbolic function. This function is obtained by fitting experimental values through a trial and error method from Oppel's numerical simulations, according to the equation:

$$\varepsilon_{eff} = \frac{A}{N} + B \tag{1}$$

where $A = \frac{\varepsilon_{eff}^{in} - 1}{1 - 1/Ntot}$; N and N_{tot} are the slab number and total number of finite elements or slabs in the numerical model and $B = \varepsilon_{eff}^{in} - A$. In spite of the apparently general expression of Eq. (1), we have to take into account that it was obtained by choosing a fixed number of 20 finite elements since this was the number of thermocouples

available in the experimental tank. To our opinion, fixing the number of finite elements to the number of available experimental gauges is not a very accurate approach from the numerical point of view and therefore we are not very confident about the simulations results and so we are about Eq. (1). As for ε_{eff}^{in}, Zurigat et al. [1] obtained mathematical correlations as a function of Reynolds (*Re*) and Richardson (*Ri*) numbers ratio, with different parameter values depending on the inlet configuration:

$$\varepsilon_{eff}^{in} = K\left(\frac{Re}{Ri}\right)^{n} \text{ with } n < 1 \tag{2}$$

Oppel [6], calculated *Re* and *Ri* as function of mean tank velocity and used tank diameter and height as the corresponding characteristic lengths. However Zurigat et al. [1] calculated these numbers in terms of velocity and hydraulic diameter of tank inlet for *Re* and inlet velocity and tank height as characteristic length for *Ri*. Taking into account that what we are looking at the ratio of the degree of turbulence introduced at the inlet (depicted by *Re*) and the turbulence suppression (depicted by *Ri*), we think that these dimensionless numbers should be referred to inlet velocity and dimensions. In Eq. (2), the effect of the inlet configuration is considered by the coefficients *K* and *n*, which were obtained by Zurigat et al. [1] from the fitting of experimental results from tanks with different inlet configurations. A set of *K* and *n* values was obtained for each kind of inlet, but no correlation was established between these values and the general inlet configuration or geometry.

Al-Najem et al., from Kuwait University [2], proposed a similar approach. They expressed the thermal equation in dimensionless coordinates and introduced turbulence and mixing effects through a parameter called *S* (see Table 1). This parameter depends on tank Peclet number (*Pe*), a turbulent mixing factor, ε, whose value is zero for laminar flow:

$$S = \frac{Pe_{tank}}{1+\varepsilon} \tag{3}$$

Similarly to Zurigat et al. [1], they observed that *S* parameter that better fitted the experimental results varied along the tank length decreasing its value from the inlet location. However these authors did not propose any specific mathematical formulation for such variation.

Nelson et al., from Indian Institute of Technology Madras [3, 4], on their side, defined a mixing coefficient, *Z*, whose expression was similar to the one defined by Zurigat et al. [1] for ε_{eff}^{in} (see Table 1). This *Z* coefficient attained a minimum value of 1, when the inlet stream and the stored fluid did not mix with each other so that the tank is perfectly stratified. Nelson et al. implemented *Z* factor in a numerical model [3] through the boundary conditions and its value was adjusted to fit the experimental results performed under different conditions. The authors claimed that the equation for calculating *Z* can be taken as a general expression since it was validated as well with results obtained by other authors for tanks with different kinds of diffusers. In contrast with the other authors, Nelson et al. did not consider that the mixing coefficient varied as thermocline zone moved away from the inlet.

TABLE 1. Implementation of turbulence and mixing phenomena in various simulation models.

Reference	Thermal energy equation and factors accounting for turbulence and mixing	
Zurigat et al. [1]	$\frac{\partial T}{\partial t} + v\frac{\partial T}{\partial z} = \alpha\varepsilon_{eff}\frac{\partial^2 T}{\partial z^2}$	$\varepsilon_{eff} = \text{decreasing hyperbolic function}$ $\varepsilon_{eff}^{in} = K\left(\frac{Re_{inlet}}{Ri_{tank}}\right)^{n}$ with $n < 1$
Al-Najem et al. [2]	$\frac{\partial \theta}{\partial \tau} + S\frac{\partial \theta}{\partial \xi} = \frac{\partial^2 \theta}{\partial \xi^2}$	$S = \frac{Pe_{tank}}{1+\varepsilon}$
Nelson et al. [3, 4]	Energy balance to the fluid in which a mixing parameter Z is implemented	$Z = 1.68 \times 10^4 \left(\frac{Re}{Ri}\right)^{0.67}$

From this literature review we can conclude that thermocline formation strongly depends on the degree of turbulence introduced given by the ratio between potential energy (natural convection) and specific kinetic energy (forced convection). The ratio between these two effects is accounted by the *Ri* number. In this sense, some authors have observed that the initial formation of thermocline can be correlated with Froude number *Fr* [7], which the inverse of *Ri* to the square (see Appendix). This confirms that it is mainly the *Ri* number who controls the stratification and hence the thermocline initial formation. Moreover, turbulence and mixing effect is expected to decrease with the distance from the inlet port. However it is clear that there is not much agreement in how the influence of these phenomena in thermocline development can be quantified. To our opinion there is not enough scientific support to assume any of the approaches presented in literature because, on the one hand, there is a lack of

experimental data with different inlet configurations and, on the other hand, the numerical simulations used for fitting the experimental data are not reliable enough.

Therefore, in this work we will try to quantify the influence of turbulence and mixing phenomena in thermocline zone formation in order to improve the analytical model based on sigmoid functions developed at CIEMAT for single storage tanks [8], which for the moment does not take into account such phenomena. For that purpose we have analyzed experimental data found in the literature for thermocline tanks with different inlet configurations. The effect of turbulence and mixing has been evaluated with an approach based on, what we have called, eddy function that has been introduced as a correction to the fluid diffusivity. The dependence of this function with the Richardson number at tank inlet has been evaluated and discussed. However, for the moment many questions still remain open since more systematic experiments with different inlet configurations and working conditions are required.

RESULTS AND DISCUSSION

Approach for Turbulence and Mixing Quantification

CIEMAT's analytical model was developed for solving the energy thermal equation of a thermocline tank expressed in dimensionless coordinates (see Appendix):

$$\frac{\partial \phi}{\partial t^*} + v^* \frac{\partial \phi}{\partial z^*} = \frac{\partial^2 \phi}{\partial z^{*2}} \tag{4}$$

This equation was initially solved by using a numerical method [9], however, since this model did not consider turbulence phenomena, a convenient number of control volumes had to be chosen for achieving an optimum fitting of the experimental data. In a later approach, the numerical results were fitted to a logistic function so that analytical expressions for the temperature evolution with tank position at a certain time were obtained. This logistic function had two parameters: z_c^*, which indicates the position of the thermocline zone center, and β_z^*, which is the slope of the temperature curve in that position [10]. Apart from facilitating the calculations, the advantage of having analytical solutions is that the parameters can be expressed in terms of physical values. However in this case, since the logistic function was obtained from numerical calculations, the variation of the sigmoid slope was parametrized by graphical fitting. In a more recent work an algebraic sigmoid [8] has been chosen as analytical function. This sigmoid has also two parameters (z_c^* and β_z^*) and its expression for the temperature evolution in dimensionless coordinates is:

$$\phi = \left\{ 1 + \frac{(z^* - z_c^*)}{\left[\frac{1}{4\beta_z^{*2}} + (z^* - z_c^*)^2 \right]^{1/2}} \right\} \tag{5}$$

Similarly to what we did in a previous work [8], experimental data of thermocline tanks with water reported by different authors [1, 2, 11, 12, 13, 14] have been fitted to Eq. (5). From the fitting, the slope values, β_z^*, at different tank axial positions, z_c^*, have been obtained. Figure 1 shows as example the fitting of one set of experimental data reported by Wildin et al. [11]

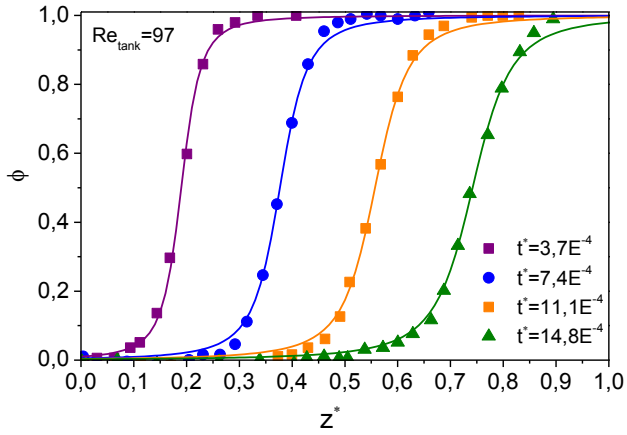

FIGURE 1. Algebraic sigmoid fitting the experimental data of Wildin et al. [11] with Re_{tank}=97.

The main features of the tanks and the relevant experimental conditions of the data analyzed are recorded in Table 2. As we can see, these tanks have different inlet configurations and work under different flow rates and temperature intervals.

TABLE 2. Tank characteristics and experimental conditions of the data analyzed in this work.

Reference	Tank dimensions	Inlet configuration	$\dot{q}$ (l/min)	T_{max}-T_{min}
Zurigat et al. [1]	L=1.44 m; D=0.4064 A= 0.1297 m^2	Side inlet Perforated inlet Impingement inlet	4.01 5.72 5.92	50ºC-25ºC
Windin et al. [11]	L=0.91 m; A= 2.40 m x 0.91 m =2.18 m^2	Diffuser in an inner circular pipe with drilled holes and an outer rectangular box. Two different opening heights	10.71-43.42	23ºC-11ºC
Al-Najem et al.[2]	L=1 m; D= 0.3 m A= 0.0707 m^2	Single port distributor with a circular mesh below	3-15	70ºC-22ºC
Karim et al. [12]	L=1.85 m; D= 0.85 m A= 0.5675 m^2	Octagonal diffuser	4.2-8	16ºC-5ºC
Gajbhiye et al.[13]	L=1 m; D= 0.485 m A= 0.1847 m^2	Two concentric perforated pipes along tank height	2.02	80ºC-30ºC
González et al. [14]	L=1.8 m; D=0.8 A= 0.5026 m^2	Conical diffuser Inlet elbow	6-16	52ºC-20ºC

As said above, the advantage of having analytical solutions is that the parameters can be expressed in terms of physical values. In the literature we can find analytical models for thermocline tanks developed by different authors that result in sigmoid functions as solutions and all of them provide expression for calculating the variation of the slope with time or tank position [15, 16, 17, 18]. We have verified that these expressions are quite similar and lead to almost the same slope values. This is because all analytical solutions found in the literature assume a laminar flow and do not consider the occurrence of turbulences and mixing at tank inlet. From all the expressions found in the literature for calculating the slope, we have chosen the one obtained by Chung et al. [18] because they propose a symmetric sigmoid function as analytical solution. The expression for calculating this slope in dimensionless coordinates is:

$$\beta^*_{z\,Chung} = \frac{3L}{4\sqrt{6\alpha t}} = \frac{3L}{4\sqrt{6\alpha z/v}} \tag{6}$$

As we can see the slope of the sigmoid depends on thermal diffusivity and decreases with time or position as a function of $1/\sqrt{t}$. Note that the presence of tank height, L, only converts the slope to dimensionless form. However the slope value tends to infinite when time or position tends to zero. This is due to the temperature step boundary condition imposed for the beginning of the dynamic processes, which implies a laminar regime for the whole process. In Fig. 2 the slope calculated with Eq. (6) ($\beta^*_{z\,Chung}$) is compared with the slope values obtained from fitting the different experimental data ($\beta^*_{z\,Exper}$). The slope variation has been represented as a function of time so that a unique curve for Chung's slope is required and experiments performed at different velocities can be compared together. In the graphs, the experimental data have been labeled with the corresponding values of Re_{tank} calculated according to the expression recorded in the Appendix. In all cases, and as expected when turbulence and mixing have certain influence, the experimental slopes are smaller than the values calculated with Eq. (6), i.e., the thermocline zone is wider than expected assuming laminar flow, as Chung's model does.

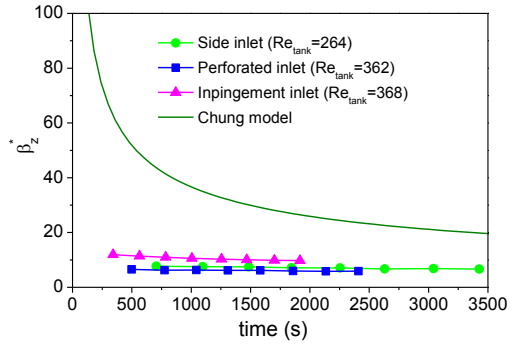

(a) Zurigat et al. [1]

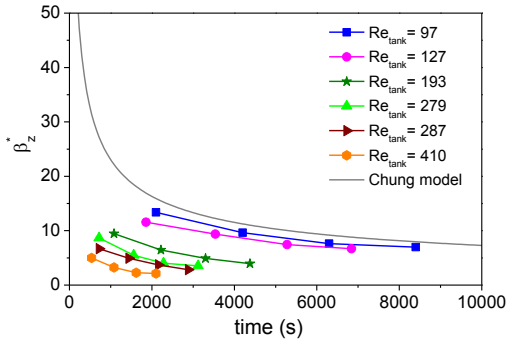

(b) Wildin et al. [11]

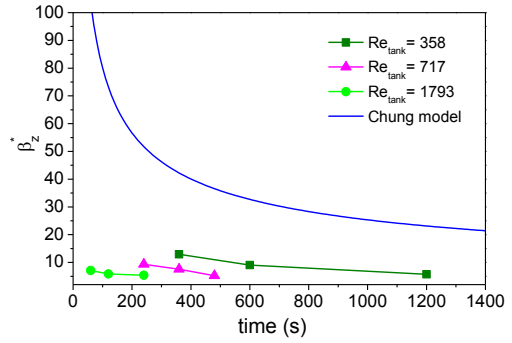

(c) Al-Najem et al.[2]

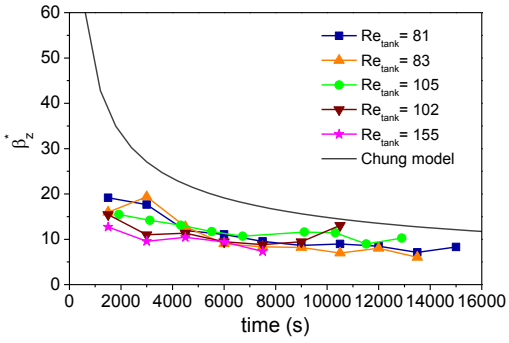

(d) Karim et al. [12]

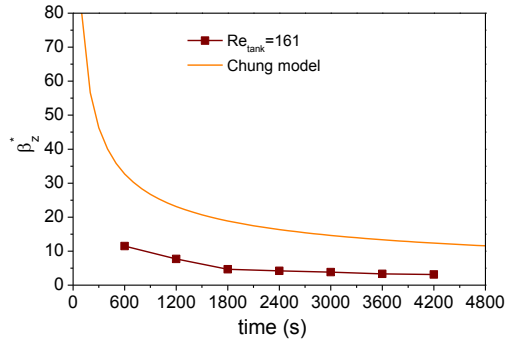

(e) Gajbhiye et al. [13]

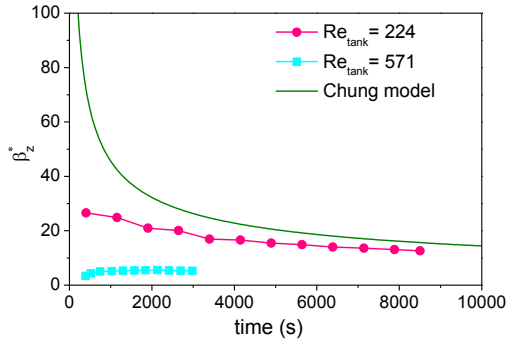

(e) González et al. [14]

FIGURE 2. Variation of sigmoid slopes with time for the analyzed experimental data. Comparison between the values obtained from the fitting and the calculated with Chung model.

Therefore, similarly to Zurigat et al. [1] and Al-Najem et al. [2], we want to introduce a factor that takes into account fluid mixing and turbulences occurring at tank inlet during dynamic processes. Both approaches are quite similar and consider a correction to the diffusivity, α. The only difference is that the parameter accounting for turbulence mixing is equal to zero (Al-Najem) or equal to 1 (Zurigat) when the flow is laminar. In both cases the authors expect the factor to vary with the distance to tank inlet. In our approach we have introduced an eddy function, f_{eddy}, similar to the factor ε_{eff} proposed by Zurigat [1]. This function can be considered as a correction of the diffusivity in the slope expression defined in Chung model (Eq.(6)) and can be calculated from the ratio between that slope and the slope obtained experimentally from the sigmoid fitting:

$$f_{eddy} = \left(\frac{\beta^*_{Z\,Chung}}{\beta^*_{Z\,Exper}}\right)^2 \tag{7}$$

This eddy function has been calculated for all the experimental data analyzed (see Table 2) and the resulting values are recorded in Table 3 together with the corresponding experimental conditions: Re_{tank}, Ri_{inlet}, kind of process and temperature interval, [T_{max}, T_{min}]. As we can see, all Re_{tank} values are well below 2100, which is the limiting value that ensures a laminar flow. Hence view all these tanks operate under laminar regime.

TABLE 3. f_{eddy}, Re_{tank} and Ri_{inlet} values, kind of process and temperature interval for the different experimental data analyzed.

Zurigat et al. [1]				
Re_{tank}	**Ri_{inlet}**	**f_{eddy}**	**Kind of process**	**[T_{max}, T_{min}] (ΔT)**
264	0.04	f_{eddy}(t) [90-13] (1)	Charge	[50ºC, 25ºC] (25ºC)
362	0.04	f_{eddy}(t) [120-27] (2)		
368	0.03	f_{eddy}(t) [77-10] (3)		
Wildin et al. [11]				
Re_{tank}	**Ri_{inlet}**	**f_{eddy}**	**Kind of process(*)**	**[T_{max}, T_{min}] (ΔT)**
97	1.69	1.4 (4)	Discharge	[23ºC, 11ºC] (12ºC)
193	0.46	6.5 (4)		
279	0.25	12 (4)		
127	5.67	2 (5)		
287	1.02	19 (5)		
410	0.53	45 (5)		
Al-Najem et al.[2]				
Re_{tank}	**Ri_{inlet}**	**f_{eddy}**	**Kind of process**	**[T_{max}, T_{min}] (ΔT)**
358	No details about inlet dimensions	13	Charge	[70ºC, 22ºC] (48ºC)
717		35		
1793		f_{eddy}(z) [200-100]		
Karim et al. [12]				
Re_{tank}	**Ri_{inlet}**	**f_{eddy}**	**Kind of process**	**[T_{max}, T_{min}] (ΔT)**
81	0.27	3	Discharge	[16ºC, 5ºC] (11ºC)
83	0.25	3	Charge	
102	0.17	4	Charge	
105	0.16	4	Discharge	
155	0.075	7	Discharge	
Gajbhiye et al.[13]				
Re_{tank}	**Ri_{inlet}**	**f_{eddy}**	**Kind of process**	**[T_{max}, T_{min}] (ΔT)**
161	No details about inlet dimensions	15	Charge	[80ºC, 30ºC] (50ºC)
González et al.[14]				
Re_{tank}	**Ri_{inlet}**	**f_{eddy}**	**Kind of process**	**[T_{max}, T_{min}] (ΔT)**
224	0.02	f_{eddy}(z) [7-1.5] (6)	Charge	[52ºC, 20ºC] (32ºC)

*Charge: hot water entering from tank top, discharge: cold water entering from tank bottom

1: side inlet, 2: perforated inlet, 3: impingement inlet, 4: 0,609-inch opening height, 5: 1 inch-opening height, (6): conical diffuser

In general, we observe that eddy function has a constant value which increases as Re_{tank} increases for the same tank and hence for the same inlet configuration. This is the case for Wildin et al. [11], Karim et al. [5], Gabjhiye et al. and Al-Najem et al. [2]. Actually, since all Re_{tank} values indicate that we should be in the laminar regime, a slope variation similar to the given by Chung's expression should be obtained and in some cases it is almost like this. However in other cases, the eddy function takes very high values and strongly depends on tank position: Al-Najem tank when Re_{tank}=1793, González tank [14] and Zurigat tank [1] (see Table 3).

As said in the Introduction, we should expect that inlet Richardson number together with the inlet configuration and geometry determines the influence of turbulences and mixing in thermocline formation and hence on the eddy function. For calculating Ri_{inlet}, the corresponding expression recorded in the Appendix has been used. The velocity v_{in} can be obtained from the known volumetric flow rate and the total diffuser flow area. $\Delta\rho$ is the density variation of the fluid in the temperature range of the experiment and ρ_m is the density at mean temperature. As characteristic length (h) a value of two times the nominal inlet diameter has been assumed, in accordance with the rough estimation of kinetic energy dissipation distance for a pipe/diffuser [20]. In Table 3 the values corresponding to some of the experimental data have been recorded. In the other cases the authors do not give details about inlet geometry and hence Ri_{inlet} could not be calculated accurately.

In general, we can say that eddy function has a constant value which increases as Ri_{inlet} decreases. In Fig. 3 we have represented this variation for Wildin et al. [11] and Karim et al. [12] results so we can see more clearly how the kind of eddy function evolution with this dimensionless number is. Actually, at low Ri_{inlet}, turbulent mixing at the inlet is dominant and the inlet configuration is more important, however at high Ri_{inlet}, high buoyancy forces inhibit mixing at the inlet region and the inlet configuration contributes less to the thermocline development [19]. Therefore since eddy function accounts for turbulence phenomena, it is expected to have higher values for lower Ri_{inlet} values. Unfortunately, since the tanks analyzed do not have the same inlet diffuser configuration (see Table 2), it is not possible to obtain a general correlation between the eddy function and Ri_{inlet} number.

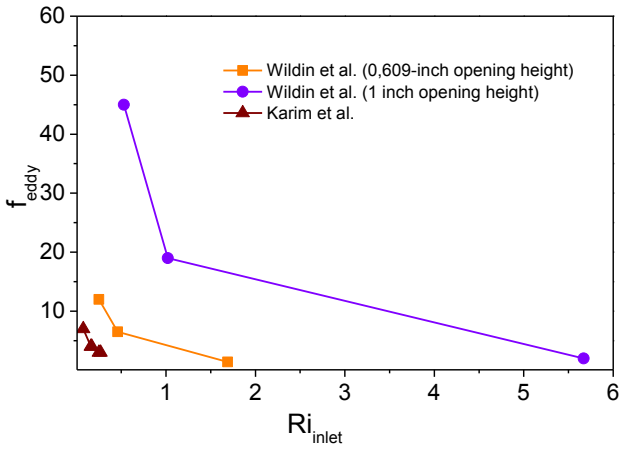

FIGURE 3.: Variation of eddy function (f_{eddy}) with inlet Ri_{inlet} number for experimental data from Wildin et al. [11] and Karim et al. [5].

The experiments of Zurigat et al. [1] and González et al. [14] seem to indicate that when Ri_{inlet} is very low, eddy function takes high values and depends on the distance from tank inlet, z. This means that when turbulences are very high, forced convection predominates over natural convection. For these cases we have used a decreasing curve for fitting the eddy function values calculated from the experimental results. The general expression for this decreasing curve is the following function with three parameters:

$$f_{eddy}(z) = 1 + \frac{K}{(z+c)^{n}} \tag{8}$$

The advantage of using this expression for fitting the experimental results is that it approaches to 1 as z increases. In this sense it is similar to the decreasing function proposed by Zurigat et al. [1]. The parameters leading to the best fitting of the experimental results are displayed in Table 4.

TABLE 4. Eddy function parameters for the different experimental data analyzed in this work.

Reference	Inlet kind	K	n	c
Zurigat et al. [1]	Side inlet	11.50	4/5	2.27×10^{-4}
	Perforated inlet	22.00	4/5	6.10×10^{-4}
	Impingement inlet	7.40	4/5	6.09×10^{-4}
González et al. [2]	Conical diffuser	0.68	4/5	2.08×10^{-4}

In all cases we obtained the same value of 4/5 for the *n* parameter. For the case of the parameter *c*, which allows having a value different from infinite for *z*=0, we have chosen the value of the mean flow velocity because it defines a *z* step for a time step of 1 second. Figure 4 displays the fitting of f_{eddy} values obtained from the experimental results of Zurigat et al. [1] with the expression of Eq. (8). As we can see, the fitting is quite good although it would be more accurate if slope data for tank positions lower that 0.2 m were available.

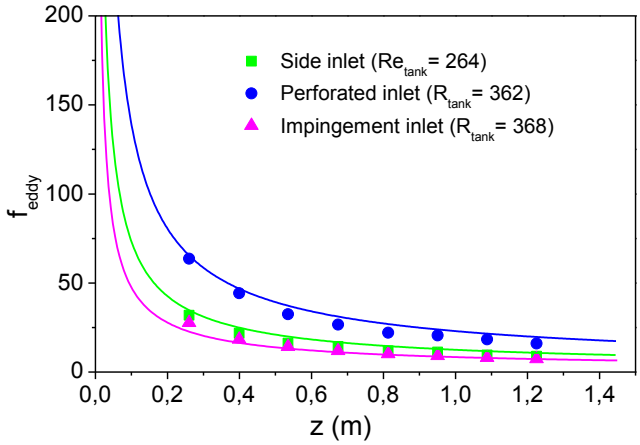

FIGURE 4.: Variation of f_{eddy} with tank position, *z*, for the experiments performed by by Zurigat et al. [1] with different inlet configurations.

Implementation of f_{eddy} in CIEMAT's Analytical Model

Once the eddy function is defined, either as constant value or as an equation that depends on the distance to tank inlet, it can be implemented in Eq. (7) so that the variation of the sigmoid slope can be calculated as:

$$\beta_z^* = \frac{\beta_{z\,Chung}^*}{\sqrt{f_{eddy}}} \tag{9}$$

In Fig. 5 we have plotted the variation of the calculated β_z^* with *z* for the experiments of Wildin et al. [11] (a) and for the experiments of Zurigat el al. [1] (b). As we can see, the calculated curves either in the case of constant eddy function or in the case of z-dependent, fit quite well the slopes experimentally obtained. Therefore thanks to this curves, we could be able to predict the thermocline formation and subsequent evolution as it moves away from the tank inlet.

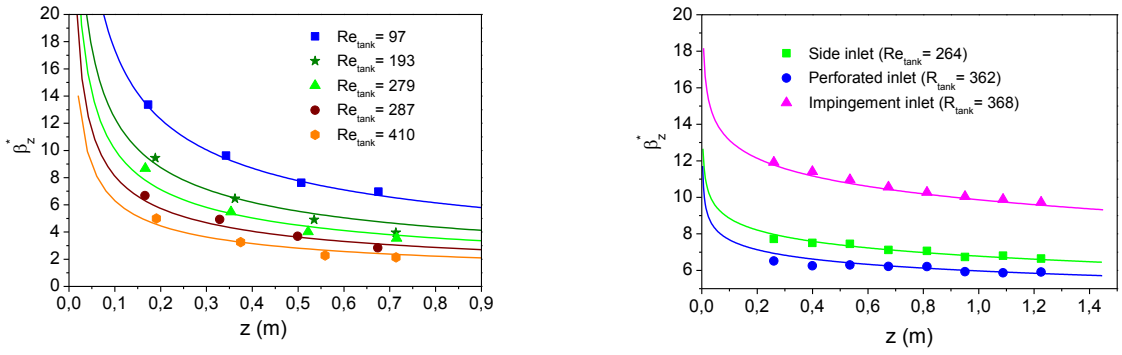

(a) (b)

FIGURE 5.: Variation of dimensionless slope (β_z^*) with tank position, *z*, for the experiments performed for some of the experiments performed by Wildin et al. [11] (a) and for the experiments performed by Zurigat et al. [1] (b) with different inlet configurations.

CONCLUSIONS

This paper intends to find out a way to predict the effects of turbulence and mixing in the initial development of the thermocline region in a single storage tank with a liquid. All with the aim of improving the analytical model based on sigmoid functions developed at CIEMAT for thermocline tanks, which still does not take into account these phenomena.

A previous literature review has been done in order to check the different approaches done by other authors for evaluating turbulence and mixing effects. Among all of them we have chosen one that accounts for turbulence and mixing phenomena by introducing a correction to the fluid diffusivity. This correction has been obtained by analyzing experimental data found in the literature for thermocline tanks with different inlet configurations. In this way the effect of turbulence and mixing has been quantified by means of an eddy function, which either takes a constant value or varies with the distance to tank inlet depending on the inflow jet characteristics. These characteristics are defined by its momentum (through the Froude or Richardson number) and its direction and position (through experimental constants).

Although the correlations proposed for the eddy function are able to fit some of the analyzed results from previous works, more systematic experiments with different inlet configurations and working conditions should be required in order to obtain general correlations between the eddy function and the inlet characteristics.

APPENDIX

L	tank height
D_H	hydraulic tank diameter
A	cross section area of the tank
d_H	hydraulic diameter of than inlet
h	characteristic length for Ri number ~ distance of turbulence influence
A_{in}	cross section inlet area
$\dot{q}$	volumetric flow
$v = \frac{\dot{q}}{A}$	mean flow velocity
$v = \frac{\dot{q}}{A_{in}}$	inlet velocity
ρ_m	density at mean temperature
μ_m	viscosity at mean temperature

$T_m = \frac{T_{max} - T_{min}}{2}$	mean temperature
$\phi = \frac{T - T_{min}}{T_{max} - T_{min}}$	dimensionless temperature
$z^* = \frac{z}{L}$	dimensionless height
$t^* = \frac{\alpha t}{L^2}$	dimensionless time
z_c^*	dimensionless thermocline position at a certain time
$Pe = \frac{Lv}{\alpha}$	tank Peclet number
$Re_{tank} = \frac{\rho_m D_H v}{\mu_m}$	Reynolds number of the tank
$Ri_{in} = \frac{g\Delta\rho h}{\rho_m v_{in}^2}$	Richardson number of tank inlet

ACKNOWLEDGMENTS

The authors would like to acknowledge the E. U. through the H2020 Program for the financial support of this work under the POLYPHEM project (Small-Scale Solar Thermal Combined Cycle) with contract number 764048 and the "Comunidad de Madrid" and European Structural Funds for their financial support to ACES2030-CM project (S2018/EMT-4319).

REFERENCES

1. Y. H. Zurigat, P. R. Liche, and A. J. Ghajar, Int. J. Heat Mass Transf. **34(1)**, 115–125 (1991).
2. N. M. Al-Najem, A. M. Al-Marafie, and K. Y. Ezuddin, Int. J. Energy Res. **17,** 77–88 (1993).
3. J. E. B. Nelson, A. R. Balakrishnan, and S. Srinivasa Murthy, Int. J. Energy Res. **22(10)**, 867–883 (1998).
4. J. E. B. Nelson, A. R. Balakrishnan, and S. Srinivasa Murthy, Int. J. Refrig. **22(3)**, 216–234 (1999).
5. A. Karim, A. Burnett, and S. Fawzia, Energies **11(5)**, 1049 (2018).
6. F.J. Oppel, M.S. Thesis Oklahoma Univ. (1985)
7. J. Yoo, M. W. Wildin and C. R. Truman, ASHRAE Trans. **92(2)**, 280-282 (1986)
8. R. Bayón and E. Rojas, AIP Conf. Proc. **2013**, 090002 (2018).
9. R. Bayón and E. Rojas, Int. J. Heat Mass Transf. **60**, 713–721 (2013).
10. R. Bayón and E. Rojas, Int. J. Heat Mass Transf. **68**, 641–648 (2014).
11. M. W. Wildin and C. W. Sohn, Fow and temperature distribution in a naturally stratified thermal storage tank. USACERL Technical Report 94/01 (1993)
12. A. Karim, Int. J. Mechanical, Aerospace, Industrial, Mechatronic and Manufacturing Eng. **3(5)**, 521–529 (2009).
13. P. Gajbhiye, N. Salunkhe, S. Kedare, M. Bose, Solar Energy **162**, 28–35 (2018)
14. P. González, Appl. Thermal Eng. **84(5)**, 196–205 (2015)
15. M. Riaz, J. Heat Transf.**99,** 489–492 (1977)
16. A. Cabelli, Sol. Energy **19**, 45–54 (1977)
17. H. Yoo, EE-T. Pak, Sol. Energy **56,** 315–322 (1996)
18. J. C. Chung and Y. Shin, Sol. Energy **85**, 3010–3016 (2011).
19. Y. H. Zurigat, A. J. Ghajar and P. M. Moretti, Appl. Energy **30**, 99–111 (1988).
20. M. Blanco, M.S. Thesis Univ. Carlos III (2010)